Radiosynthesis of Carbon-11 Labelled Puromycin as a Potential PET Candidate for Imaging Protein Synthesis *In Vivo*.

Selena Milicevic Sephton*, Franklin I. Aigbirhio

Molecular Imaging Chemistry Laboratory, Wolfson Brain Imaging Centre, Department of Clinical Neurosciences, University of Cambridge, Box 65, Cambridge Biomedical Campus, Hills Road, Cambridge, UK, CB2 0QQ.

Positron Emission Tomography, Puromycin, Rate of Protein Synthesis.

ABSTRACT: In order to address the limitations associated with the present range of PET radiotracers used for imaging protein synthesis *in vivo* we have synthesised a candidate PET radiotracer based on Puromycin (**3**, PURO), a protein synthesis inhibitor. The desmethylPURO **9** precursor for radiolabeling with carbon-11 radioisotope, was synthesized in two steps employing EDC/HOBt amide coupling in overall 76% yield. Optimal conditions for radiolabelling were then established *via* methylation/deprotection sequence. Under these condition as determined by NMR analysis **9** showed partial stability (ca. 80%) under acidic conditions. Limited evidence of stereochemical stability of **3** was also found. The radiolabelling of intermediate [^{11}C]**12** was accomplished with up to 57% conversion from [^{11}C]iodomethane. An automated method was then developed for high radioactivity radiosynthesis to produce [^{11}C]**3** ([^{11}C]PURO) in 16±6% (n=3) decay corrected radiochemical yields.

The rate of protein synthesis (RPS) which represents one of the hallmarks of cancer, is a target for imaging with positron emission tomography (PET). To image RPS *in vivo*, protein building blocks, amino acids for example, radiolabelled with PET radionuclides (e.g., fluorine-18; $t_{1/2}$ = 109.8 min or carbon-11; $t_{1/2}$ = 20.4 min) have been employed extensively.[1]

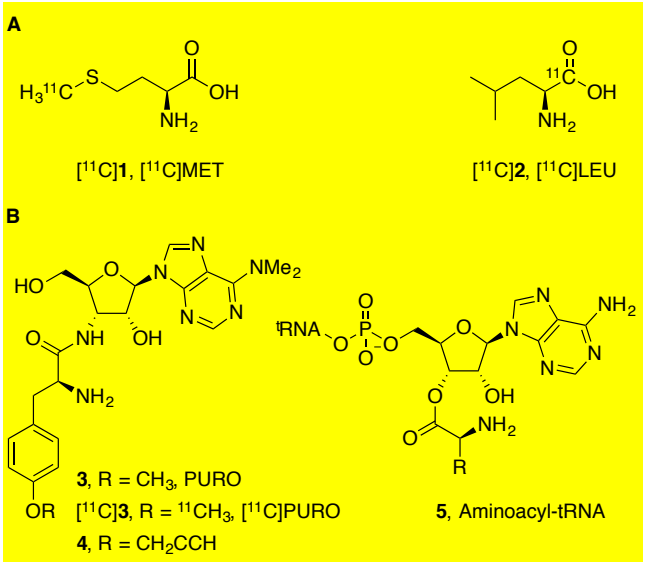

Chart 1. (A) Structures of most commonly employed amino acids for PET imaging of protein synthesis and (B) Structures of Puromycin derivatives and aminoacyl-tRNA.

To date, the most commonly used amino acid for PET imaging is [^{11}C]-Methionine ([^{11}C]**1**, [^{11}C]MET, Chart 1).[1,2] The radiolabelling of [^{11}C]**1** is straightforward and [^{11}C]**1** is successful in crossing the blood brain barrier (BBB). The highest accumulation of [^{11}C]**1** was found in the organs with the highest rate of protein synthesis *in vivo*: brain, liver and pancreas.[3] Although PET imaging with radiolabelled amino acids is routinely used, quantification of the PET data is complicated due to amino acid involvement in other metabolic processes (e.g., amino acid active transport).[1] In 1993, a study compared three radiolabelled amino acids: [^{3}H]**1**, [^{18}F]Tyrosine ([^{18}F]TYR, structure not shown) and [^{14}C]Leucine ([^{14}C]**2**, [^{14}C]LEU, Chart 1)[4] for their ability to image protein synthesis *in vivo*. The authors found that the rate of protein synthesis was reduced in brain and pancreas only with [^{14}C]**2** under blocking conditions using the protein synthesis inhibitor cycloheximide in excess amounts. Subsequently, [^{11}C]**2** emerged as a superior PET radiotracer for imaging protein synthesis *in vivo*,[5,6,7] however it is not without limitations. Amino acid [^{11}C]**2** is radiolabeled with the short-lived carbon-11 and the radiosynthesis is lengthy and challenging. This is primarily because it requires carbon-11 HCN which is not readily available from the cyclotron.[8,9] In addition, the

radiosynthesis requires chiral prep-HPLC separation to obtain the L-form from the crude mixture. Furthermore, quantitative PET analysis requires arterial blood sampling coupled with metabolite analysis which involves trapping and measuring of gaseous [^{11}C]CO_2 radiometabolite.[10]

In order to overcome difficulties associated with the PET analysis using amino acid based radiotracers, our group sought to explore a potential PET radiotracer based on the Puromycin (**3**, PURO, Chart 1) scaffold.[11] Amide **3** is an aminonucleoside antibiotic from *Streptomyces albo-niger*, and a protein synthesis inhibitor. As such, **3** exhibits inhibitory activity *via* the covalent attachment to the nascent protein chains.[12,13,14] Eukaryotic ribosome can then insert **3** (PURO) in place of aminoacyl-tRNA (**5**, Chart 1) causing premature termination of translation, resulting in truncated proteins. The concept of imaging protein synthesis *in vivo* using protein synthesis inhibitor has been employed previously.[15] In 2012, the Salic group[16] employed **4**, (*O*-PropagylPURO, Chart 1) and fluoresence imaging was accomplished *via* the [2+3] cycloaddition between **4** and fluorophore tagged azide. The authors were successful in establishing that protein synthesis was indeed inhibited as quantified by fluorescence measurement in cultured cells as well as *ex vivo*.

To assess this concept for imaging RPS *in vivo* by PET we selected [^{11}C]**3** (*O*-carbon-11 labeled **3** (PURO), Chart 1) as a potential radiotracer candidate. In analogy to fluorescence imaging with **4**,[16] the concept of a PET PURO radiotracer would be based on accumulation of radioactivity from [^{11}C]**3** within the ribosome which can then be visualized and quantified by PET. However, several challenges were considered in the design and synthesis of [^{11}C]**3** arising from the chemical scaffold of **3** having the following features: five stereocentres, three reactive exchangeable functional groups (two hydroxyl and one amine) and one labile amide bond. Herein, we report the synthesis of a respective precursor for the radiosynthesis of [^{11}C]**3**, NMR experimental evidence for its chemical and stereochemical stability as well as carbon-11 modular radiosynthesis of [^{11}C]**3**.

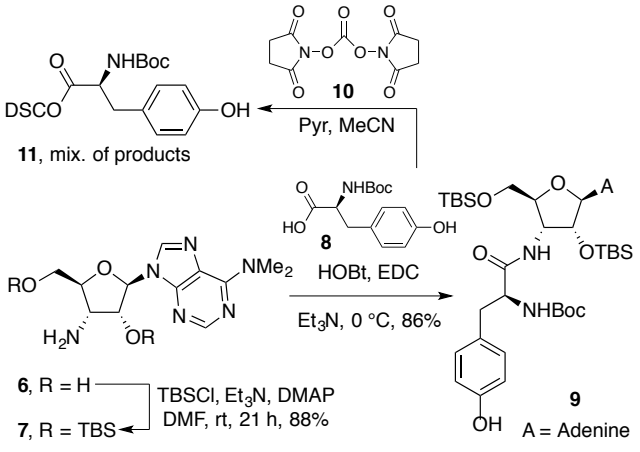

Scheme 1. Concise synthesis of common intermediate/precursor 9 for derivatization of 3 and radiosynthesis of [^{11}C]3.

The required desmethylPURO radiolabelling precursor phenol **9** (Scheme 1) also has an advantage of being a common intermediate for further derivatization of **3**.[17,18] In their synthesis of **4**, Salic and co-workers used commercially available puromycin aminonucleoside (**6**, Scheme 1) and utilized a disuccinimidyl (DSC) ester coupling (not shown) to form the critical amide bond in the framework of **3**.[16] In the synthesis of **9**, tyrosine **8** was initially used to form the corresponding DSC ester **11**. However, with the more reactive free phenol functionality in the molecule, only a mixture of inseparable products was obtained. Faced with the complications with the DSC ester coupling method, we revisited the synthesis of the **3** (PURO) manifold[17,18] and developed a two-step synthesis of **9** as depicted in Scheme 1. The two hydroxyl groups in **6** were protected with TBS to facilitate the subsequent amide coupling by avoiding side reactions observed when unprotected **6** was employed. Only a modest 30% yield of **9** was reached when unprotected **6** was employed for the coupling directly. Similarly, protected precursor **9** is less likely to undergo side reactions during radiolabelling. In the second step TBS-protected aminonucleoside **7** was coupled to commercially available Boc-protected tyrosine **8** using HOBt/EDC coupling conditions[19] to afford **9** in 86% yield.

Table 1. Conditions for the non-radioactive methylation of desmethylPURO

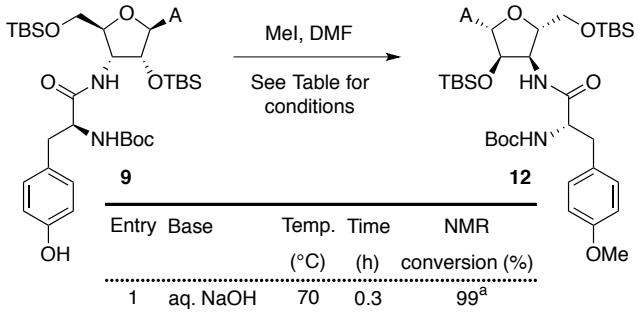

Entry	Base	Temp. (°C)	Time (h)	NMR conversion (%)
1	aq. NaOH	70	0.3	99[a]
2	aq. NaOH	90	0.1	84
3	K_2CO_3	RT	20	33
4	K_2CO_3	70	1	73
5	**aq. K_2CO_3**	**70**	**0.3**	**82**
6	aq. K_2CO_3[b]	70	1	18
7	NaH	RT	20	mix
8	aq. TBAOH	70	0.3	mix

[a] Very low mass recovery (ca. 50%); [b] Reaction done in MeCN as solvent;

With **9** in hand, we next explored conditions for methylation of the phenolic functionality in **9** (Table 1) which could then be translated to the radiosynthesis. Several bases were investigated (entries 1-8), with NaOH (entries 1 and 2) and K_2CO_3 (entries 3-6) showing good conver-

sions to product. However, with NaOH at 70 °C and 90 °C, low mass recovery (50%) was found or the conversion to product was lower, respectively (entries 1 vs. 2). To avoid the possibility of racemization with NaOH, further optimization of conditions was conducted with K_2CO_3 and showed higher yield with higher reaction temperature but shorter reaction time (entry 3 vs. 4 and 5). The yield was significantly reduced with MeCN as solvent (entry 6) and interestingly an aqueous solution of K_2CO_3 yielded 82% of **12** (entry 5). A homogeneous reaction mixture was particularly well suited for automation of radiolabelling procedure.

In order to establish optimal reaction conditions for removal of TBS and Boc protecting groups in one step, acidic hydrolysis of **12** was investigated. Complete decomposition, particularly seen through cleavage of the amide bond was observed when **12** was treated with 2 M aq. HCl for 1 h at either 100 or 80 °C. Similarly **12** decomposed upon treatment with 1.25 M methanolic HCl at 60 °C over 1 h as well as at ambient temperature over 30 min. Initial failed attempts to achieve complete deprotection of **12** prompted us to investigate acidic hydrolysis in an NMR experiment using a DCl/D_2O/MeOD-d_4 mixture with **12**. Successful monitoring of the reaction progress was dependent on the solubility of **12**, which dissolved only partly in DCl/D_2O for which reason MeOD-d_4 was added to ensure solubility was complete. The mixture was heated to 70 °C and NMR analysis performed at intervals indicated in Table 2. An unidentified by-product was observed and accounted for in molar ratios with starting material (SM), product and by-product. SM was consumed within 30 min (entries 1-3) and the amount of by-product increased with time (entries 1-4). After 10 min (entry 1) there was 37% of product and 9% of by-product and this ratio changed to 42% product and 35% by-product after 20 min (entry 2). With time more SM was consumed, but the relative amount of desired product did not improve. For this reason 10 min was set as the optimal reaction time. Although the NMR data showed no change in chemical shifts for the desired product once formed (see Supporting Information), actual ratios of SM:product:by-product suggested partial instability of **3** (entry 3 vs. 4).

Table 2. Time dependent experiments for the one step deprotection to obtain 3 (NMR monitored)

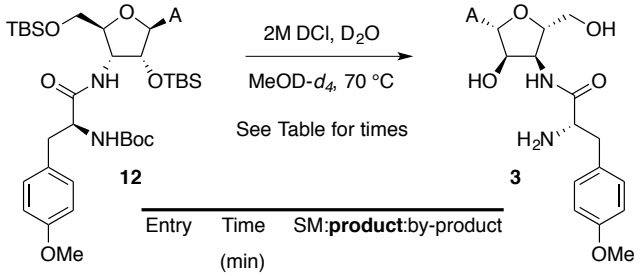

Entry	Time (min)	SM:**product**:by-product
1	10	62:**42**:10
2	20	10:**19**:16
3	30	0:**10**:14
4	60	0:**10**:22

Both TBS and Boc protecting groups were removed in a single step with aqueous hydrochloric acid; however further NMR experiment was required to confirm the stereochemical identity and determine stability of formed product **3**.

Table 3. Comparison of commercially available 3 and synthesized radiolabelling intermediate 12 in one-step hydrolysis (NMR monitored)

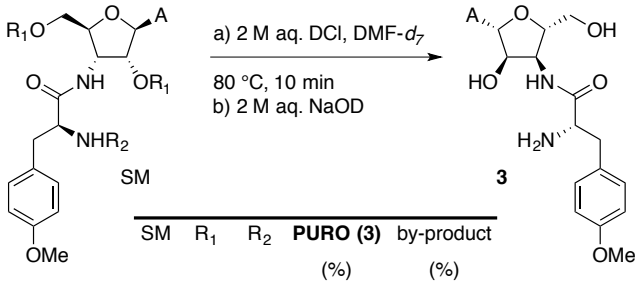

SM	R_1	R_2	**PURO (3)** (%)	by-product (%)
3	H	H	82	18
12	TBS	Boc	77	23

Both commercially available **3** and fully protected intermediate **12** were treated with 2 M aq. DCl in DMF-d_7 at 80 °C for 10 min and then neutralized with aq. NaOD and subjected to analysis by NMR (Table 3). These reaction conditions were selected considering two requirements for the choice of solvent. Methylation step was performed in DMF (**9** to **12**, Table 1) and the deprotection under radiochemical conditions was foreseen without previous removal of DMF from the reaction mixture. Also, suggested instability of **3** (Table 2) could likely be due to the presence of protic solvent (MeOD-d_4). Analysis of NMR spectral data revealed 82% intact sample after the treatment of **3** with acid. Gratifyingly, under the same hydrolysis conditions **12** afforded 77% desired product identical to commercially available **3** when comparing corresponding chemical shifts. The NMR data also indicated presence of by-product in 18% and 23% from **3** and **12**, respectively (Table 3). This strongly suggests that although the removal of TBS and Boc protecting groups yielded **3**, under acidic conditions **3** was partly chemically unstable. Due to minimally different chemical shifts amongst epimers of **3**[18]

stereochemical identity of formed **3** could not be unambiguously determined by NMR despite good chemical shift agreement between synthesized **3** and that commercially sourced. However, a doubling of peaks would be expected should epimerization occur and this was not observed.

Table 4. Radiochemistry of 9 (desmethylPURO) to obtain [^{11}C]3

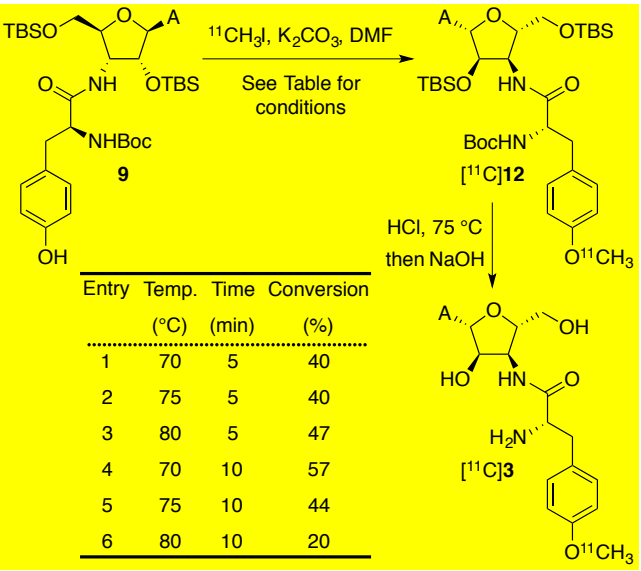

Entry	Temp. (°C)	Time (min)	Conversion (%)
1	70	5	40
2	75	5	40
3	80	5	47
4	70	10	57
5	75	10	44
6	80	10	20

Next, we explored methylation/deprotection sequence under radiochemical (i.e., *hot*) conditions. For this purpose, aq. K_2CO_3 was used and [^{11}C]iodomethane produced from cyclotron-generated [^{11}C]CO_2, was trapped in DMF and this solution was added to radiolabelling precursor **9**. To reduce the reaction time, reaction temperature was increased to 70, 75 or 80 °C (Table 4). Aliquots were analyzed by HPLC after 5 and 10 min and the results revealed no significant difference among three temperatures at 5 min (entries 1-3). Longer reaction time was proven beneficial (entries 1 vs. 4, 2 vs. 5), unless temperature was 80 °C in which case decomposition of both radiolabelled precursor and formed product was predominant (entries 3 vs 6). The deprotection step was performed under acidic conditions previously established with non-radioactive **12** (i.e., *cold*) to afford [^{11}C]**3** as confirmed by HPLC co-injection with commercially available **3**.

For initial proof of principle, development method based on [^{11}C]CH_3I trapping was sufficient to demonstrate that [^{11}C]**3** can be prepared, however automated radiosynthesis was required to enable production of [^{11}C]**3** on larger scale. We selected to use iPHASE module[20] with an attached semi-prep HPLC. The iPHASE module contains a small volume (1 mL) reactor for which reason the radiosynthesis was modified as follows; *i*) the volumes of acid and base were reduced whilst increasing their concentration (4 M vs previously used 2 M HCl and NaOH); *ii*) the reaction temperature was kept at 75 °C for both methylation and deprotection; and *iii*) the reaction time was reduced to 5 min for each step. Before injection onto semi-prep HPLC the crude reaction mixture was neutralized with aq. NaOH to ensure pH was >7. Within 70 min from the end-of-bombardment (EOB) ca. 350 MBq of [^{11}C]**3** was isolated with 66 GBq/μmol specific activity in 16±6% (n=3) decay corrected radiochemical yield and >99% radiochemical purity at end-of-synthesis (EOS).

In conclusion, we have prepared **9** (desmethylPURO precursor) in two steps from commercially available materials in 76% overall yield improving the published synthesis of similar PURO derivatives. NMR analysis of **3** and fully protected radiolabelling intermediate **12** showed partial (ca. 80%) chemical stability of **3** and limited evidence provided support for the lack of epimerization. Optimal conditions were found for non-radioactive [^{12}C]- and radioactive [^{11}C]-methylation/deprotection sequence to produce [^{11}C]**3** using [^{11}C]iodomethane. An automated method was then developed to enable preparation of [^{11}C]**3** in 16±6% (n=3) decay corrected radiochemical yield with high radiochemical purity (>99%) and specific activity of 66 GBq/μmol at EOS. The radiosynthesis of [^{11}C]**3** included a two-step radiolabelling followed by semi-preparative HPLC purification and C18 Light Sep-Pak trapping and [^{11}C]**3** was produced within 70 min from EOB. *In vitro* and *in vivo* studies are on-going in our group to evaluate [^{11}C]**3** as a potential PET radiotracer for imaging protein synthesis and will be reported in due course.

ASSOCIATED CONTENT

Supporting Information

Full experimental procedures and characterization of all compounds, results of NMR experiments, radio and UV traces for [^{11}C]**3** (PDF). This material is available free of charge on the ACS Publications website.

AUTHOR INFORMATION

Corresponding Author

* Email: sms96@wbic.cam.ac.uk

Author Contributions

All authors have given approval to the final version of the manuscript.

Notes

The authors declare no competing financial interest.

ACKNOWLEDGMENT

The authors acknowledge Dr. Lindsay McMurray (WBIC) and Mr. Robert Bielik (CRUK) for technical assistance with the production of [^{11}C]CH_3I and working with iPHASE as well as many useful discussions. Dr. Mark A. Sephton (Discovery from Charles River, UK) is acknowledged for proofreading the manuscript. NMSF (EPSRC) at the University of Swansea is acknowledged for running HRMS data.

ABBREVIATIONS

[^{11}C]MET, carbon-11 methionine; PET, Positron Emission Tomography; [^{3}H]MET, tritiated methionine; [^{18}F]TYR, fluorine-18 tyrosine; [^{14}C]LEU, carbon-14 leucine; [^{11}C]LEU, carbon-11 leucine; PURO, puromycin; *t*RNA, transcription ribonucleic acid; NMR, nuclear magnetic resonance; DSC disuccinimydil; TBS, *tert*-butyldimethylsilyl; DMF, *N,N`*-dimethylformamide; Boc, *tert*-butyloxycarbonyl; HOBt, hydroxybenzotriazole; EDC, 1-ethyl-3-(3-dimethylaminopropyl)carbodiimide; HPLC, high pressure liquid chromatography; HCN, hydrogen cyanide; EOB, end-of-bombardment; EOS, end-of-synthesis; RPS, rate of protein synthesis.

REFERENCES

(1) Jager, P. L.; Vaalburg, W.; Pruim, J.; de Vries, E. G.; Langen, K. J.; Piers, D. a. Radiolabeled Amino Acids: Basic Aspects and Clinical Applications in Oncology. *J. Nucl. Med.* **2001**, *42* (3), 432–445.

(2) Kläsner, B. D.; Krause, B. J.; Beer, A. J.; Drzezga, A. PET Imaging of Gliomas Using Novel Tracers: A Sleeping Beauty Waiting to Be Kissed. *Expert Rev. Anticancer Ther.* **2010**, *10* (5), 609–613.

(3) Shahbazian, F. M.; Jacobs, M.; Lajtha, A. Rates of Protein Synthesis in Brain and Other Organs. *Int. J. Dev. Neurosci.* **1987**, 5 (1), 39–42.

(4) Ishiwata, K.; Kubota, K.; Murakami, M.; Kubota, R.; Sasaki, T.; Ishii, S.; Senda, M. Re-Evaluation of Amino Acid PET Studies: Can the Protein Synthesis Rates in Brain and Tumor Tissues Be Measured in Vivo? *J. Nucl. Med.* **1993**, *34* (11), 1936–1943.

(5) Hawkins, R. a; Huang, S. C.; Barrio, J. R.; Keen, R. E.; Feng, D.; Mazziotta, J. C.; Phelps, M. E. Estimation of Local Cerebral Protein Synthesis Rates with L-[^{11}C]leucine and PET: Methods, Model, and Results in Animals and Humans. *J. Cereb. Blood Flow Metab.* **1989**, *9*, 446–460.

(6) Tomasi, G.; Bertoldo, A.; Bishu, S.; Unterman, A.; Smith, C. B.; Schmidt, K. C. Voxel-Based Estimation of Kinetic Model Parameters of the L-[1-^{11}C]leucine PET Method for Determination of Regional Rates of Cerebral Protein Synthesis: Validation and Comparison with Region-of-Interest-Based Methods. *J. Cereb. Blood Flow Metab.* **2009**, *29* (7), 1317–1331.

(7) Veronese, M.; Schmidt, K. C.; Smith, C. B.; Bertoldo, A. Use of Spectral Analysis with Iterative Filter for Voxelwise Determination of Regional Rates of Cerebral Protein Synthesis with L-[1-^{11}C]leucine PET. *J. Cereb. Blood Flow Metab.* **2012**, *32* (6), 1073–1085.

(8) Barrio, J. R.; Keen, R. E.; Ropchan, J. R.; Macdonald, N. S.; Baumgartner, F. J.; Padgett, H. C.; Phelps, M. E. L-[^{11}C] Leucine: Routine Synthesis by Enzymatic Resolution L-[^{11}C] Leucine: Routine Synthesis by Enzymatic Resolution. **1983**, *24* (6), 515–521.

(9) Mu, F.; Mangner, T. J.; Chugani, H. T. Facile Synthesis of L-[^{11}C] Leucine as a PET Radiotracer for the Measurement of Cerebral Protein Synthesis. *J. Label. Compd. Radiopharm.* **2005**, *48*, S189.

(10) Bishu, S.; Schmidt, K. C.; Burlin, T.; Channing, M.; Conant, S.; Huang, T.; Liu, Z.; Qin, M.; Unterman, A.; Xia, Z.; Zametkin, A.; Herscovitch, P.; Smith, C. B. Regional Rates of Cerebral Protein Synthesis Measured with L-[1-^{11}C]leucine and PET in Conscious, Young Adult Men: Normal Values, Variability, and Reproducibility. *J. Cereb. Blood Flow Metab.* **2008**, *28* (8), 1502–1513.

(11) Azzam, M. E.; Algranati, I. D. Mechanism of Puromycin Action: Fate of Ribosomes after Release of Nascent Protein Chains from Polysomes. *Proc. Natl. Acad. Sci. U. S. A.* **1973**, *70* (12), 3866–3869.

(12) Starck, S. R.; Roberts, R. W. Puromycin Oligonucleotides Reveal Steric Restrictions for Ribosome Entry and Multiple Modes of Translation Inhibition. *RNA* **2002**, *8*, 890–903.

(13) Miyamoto-Sato, E.; Nemoto, N.; Kobayashi, K.; Yanagawa, H. Specific Bonding of Puromycin to Full-Length Protein at the C-Terminus. *Nucleic Acids Res.* **2000**, *28* (5), 1176–1182.

(14) Eckermann, D. J.; Greenwell, P.; Symons, R. H. Peptide-Bond Formation on the Ribosome. A Comparison of the Acceptor-Substrate Specificity of Peptidyl Transferase in Bacterial and Mammalian Ribosomes Using Puromycin Analogues. *Eur. J. Biochem.* **1974**, *41* (3), 547–554.

(15) Eigner, S.; Vera, D. R. B.; Fellner, M.; Loktionova, N. S.; Piel, M.; Lebeda, O.; Rösch, F.; Roß, T. L.; Henke, K. E. Imaging of Protein Synthesis: In Vitro and in Vivo Evaluation of ^{44}Sc-DOTA-Puromycin. *Mol. Imaging Biol.* **2013**, *15* (1), 79–86.

(16) Liu, J.; Xu, Y.; Stoleru, D.; Salic, A. Imaging Protein Synthesis in Cells and Tissues with an Alkyne Analog of Puromycin. *Proc. Natl. Acad. Sci.* **2012**, *109* (2), 413–418.

(17) Lee, H.; Fong, K. L.; Vince, R. Puromycin Analogues. Effect of Aryl-Substituted Puromycin Analogues on the Ribosomal Peptidyltransferase Reaction. *J. Med. Chem.* **1981**, *24* (3), 304–308.

(18) Starck, S. R.; Qi, X.; Olsen, B. N.; Roberts, R. W. The Puromycin Route to Assess Stereo- and Regiochemical Constraints on Peptide Bond Formation in Eukaryotic Ribosomes. *J. Am. Chem. Soc.* **2003**, *125* (27), 8090–8091.

(19) Valeur, E.; Bradley, M. Amide Bond Formation: Beyond the Myth of Coupling Reagents. *Chem. Soc. Rev.* **2009**, *38* (2), 606–631.

(20) Ackermann, U.; Plougastel, L.; Wichmann, C.; Goh, Y. W.; Yeoh, S. D.; Poniger, S. S.; Tochon-Danguy, H. J.; Scott, A. M. Fully Automated Synthesis and Coupling of [^{18}F]FBEM to Glutathione Using the iPHASE FlexLab Module. *J. Labelled Comp. Radiopharm.* **2014**, *57* (2), 115–120.

SYNOPSIS TOC Synthesis of radiolabelling precursor desmethylPURO **9** and radiosynthesis of novel [^{11}C]**3** ([^{11}C]PURO) as a candidate for PET imaging of protein synthesis *in vivo*.

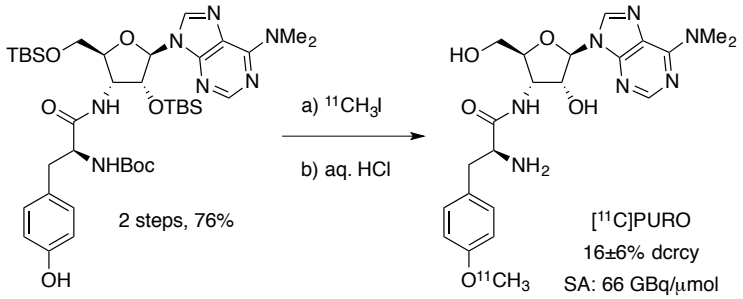

Insert Table of Contents artwork here